Perceptual Organization of Radial Symmetries *

Qing Yang
National Laboratory of Pattern Recognition
Institute of Automation
Beijing 100080, P.R. China

Bahram Parvin
Imaging and Informatics
Lawrence Berkeley National Laboratory
Berkeley, CA 94720, USA

Abstract

Radial symmetry is an important perceptual cue for the feature-based representation, fixation, and description of large-scale data sets. A new approach based on iterative voting along the gradient direction is introduced for inferring the center of mass for objects demonstrating radial symmetries that are not limited to convex geometries. The kernel topography is unique in that it votes for the most likely set of grid points where the center of mass may be located. Initially, it is applied in the direction of the gradient and then reoriented iteratively in the most probable direction. This technique can detect perceptual symmetries, has an excellent noise immunity, and is shown to be tolerant to moderate perturbation in scale. Applications of this approach to blobs with incomplete and noisy boundaries, multimedia scenes, and scientific images are demonstrated.

1. Introduction

Radial symmetry is a perceptual cue and a preattentive process [1] that improves recognition, provides an efficient mechanism for scene representation, and aids in reconstruction and description. Radial symmetry is a special class of symmetry that persists in nature at multiple scales. Its robust and efficient detection facilitates semantic representation of spatial data for summarization and interpretation. Examples include the shape of a nucleus, organization of nuclei in tissue observed with an epifluorescence microscope, oceanic vortices imaged through satellite observational platforms or numerical simulation models of fluid flow, and general blob detection. At the lowest level, a radial symmetry operator can be used as an interest operator for detecting critical features (e.g., singular events) that lead, for example, toward visual attention. However, interest operators have to be fast, retain good noise immunity, be sufficiently stable with respect to the underlying intensity distribution, and be capable of delineating/resolving nearby features into disjointed events. In this paper, the notion of circular symmetry is used in a weak sense, because the basic geometry is allowed to deviate from convexity and strict symmetry. In this sense, the center of mass could also be a perceptual event. Furthermore, our method allows the inference of the center of mass from incomplete boundary information through voting and perceptual grouping implemented through the refinement of spatially tuned voting kernels.

Spatial voting has been studied for at least four decades. Hough introduced the notion of parametric clustering in terms of well-defined geometry, which was later extended to the generalized Hough transform. In general, voting operates on the notion of continuity and proximity, which can occur at multiple scales, e.g., points, lines, lines of symmetry, generalized cylinders. The novelty of our approach is in defining a series of kernels that vote iteratively for the likelihood of the center of mass. At each iteration, the center of mass is refined until it converges to a single focal response. These kernels are cone-shaped, have a specific scale and spread, and target geometric features of approximately known dimensions. Initially, the voting kernels are applied along the gradient direction; then, at each consecutive iteration and at each grid location, their orientation is aligned along the maximum response of the voting space. The shape of the kernel is also refined and focused as the iterative process continues. We show that our approach is applicable to perceptual shape features, has an excellent noise immunity, is tolerant to variations in target shape scale, and is applicable to a large class of application domains.

This paper is organized as follows: Section 2 provides a review of the previous research. Section 3 describes the basic idea and detailed implementation of evolutionary voting. Section 4 discusses the selection of parameters and their effects on the algorithm. Section 5 demonstrates the experimental results. And section 6 concludes the paper.

* Research was funded by the Mathematical, Information, and Computational Sciences Division and the Life Sciences Division of the U. S. Department of Energy under Contract No. DE-AC03-76SF00098 with the University of California. The publication number is LBNL-54728.

2. Review of previous work

Ambiguities in detecting circular symmetries are often due to variation in scale, presence of noise, and changes in intensity distribution. These ambiguities lead to diffusion and dispersion of the locus of symmetry in the object space. Figure 1 shows variations in the shape geometry as a result of angular deviation between the gradient and radial vector that can result in ambiguity in the presence of noise.

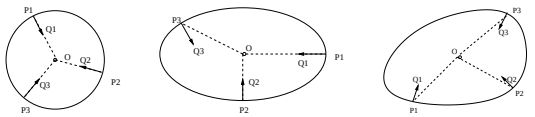

(a) (b) (c)

Figure 1. Topological variation as a result of an angular difference between the radial vector and gradient: (a) circle; (b) ellipse; and (c) general convex region.

We view radial symmetries to be a superset of circular symmetries, and in this context, the bulk of previous research has been limited to the later class. Techniques in circular symmetries can be classified into three different categories: (1) point operations leading to dense output, (2) clustering based on parameterized shape model or voting, and (3) iterative techniques. Point operations are usually a series of cascade filters that are tuned for radial symmetries [3]. These techniques use image gradient and orientation to infer the center of mass for blobs of interest [6, 7, 8]. Recent efforts [3] have focused on speed and reliability. Parametric clustering techniques are often based on a variant of the Hough transform [2], e.g., a circle or ellipse finder. These techniques produce loci of points corresponding to the parametric models of well-known geometries. These point distributions are then merged and model parameters are refined. Nonparametric clustering techniques operate along the gradient direction to search for radial symmetry, which could be line- or area-based. Line-based search [5] is also known as the spoke filter where the frequency of occurrence of points normal to the edge direction are clustered. In contrast, area-based voting accumulates votes in a small neighborhood along the gradient direction. Examples of iterative methods include watershed [9] and regularized centroid transform (RCT) [10], which iteratively transport boundary points to the local center of mass. These can be classified as curve-based voting since the voting path is not along a straight line but along a minimum energy path. Voting paths can be easily distorted by noise, local structures, and other singularities in the image, and may lead to oversegmentation. To overcome these difficulties, RCT regularizes the solution to the centroid transform [10] to eliminate inherent singularities. The technique has been demonstrated for localizing the center of mass along the minimum energy path. The main advantage of this technique is in the delineation of the overlapping objects through computation of a vector field, which also leads to simultaneous segmentation.

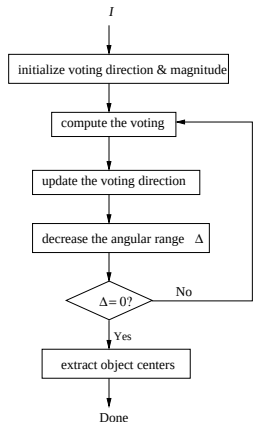

Figure 2. Operational flow for iterative voting.

In summary, interest-point operators are fast and well-suited for detecting small features for higher levels of interpretation and manipulation. Parametric voting techniques could be memory intensive depending on the dimensionality of the parameter space, and could remain sensitive to small deviation from the underlying geometric model. Line- and area-based voting produce a voting space that is diffused and subject to further ad hoc analysis. On the other hand, iterative techniques are adaptive to geometric perturbation and produce more stable results. The proposed method is also iterative and demonstrates superior performance in the presence of noise, variations in scale, and topological changes.

3. Approach

The iterative voting protocol is illustrated in Figure 2. It is initialized by voting along the gradient direction where at each consecutive iteration the voting direction and the shape of the kernel is refined. Let

- $I(x, y), (x, y) \in D$ be the original image, where D is the image domain.
- $M(x, y)$ be the voting magnitude.
- $\alpha(x, y)$ be the voting direction, where $\alpha(x, y) := (\cos\theta(x, y), \sin\theta(x, y))$.

- $r_{\min}, r_{\max}$ be the range of radial symmetry.
- the voting area be

$$A(x,y;r_{\min},r_{\max},\Delta) := \{(x \pm r\cos\phi, y \pm r\sin\phi) \\ |r_{\min} \le r \le r_{\max}, \theta(x,y) - \Delta \le \phi \le \theta(x,y) + \Delta\} \quad (1)$$

  Where the signs in the above formula are discussed later.
- the vote image with parameters $(r_{\min}, r_{\max}, \Delta)$, denoted by $V(x, y; r_{\min}, r_{\max}, \Delta)$.

The voting algorithm is as follows:

Tunable Voting

(1) *Initialize the parameters:* Choose $r_{\min}, r_{\max}, \Delta_{\max}$ and a sequence $\Delta_{\max} = \Delta_N < \Delta_{N-1} < \cdots < \Delta_0 = 0$. Set $n := N, \Delta = \Delta_{\max}$.
(2) *Initialize voting direction and magnitude:* Calculate the gradient $(I_x(x,y), I_y(x,y))$, and let $M(x,y) := \sqrt{I_x(x,y)^2 + I_y(x,y)^2}$ be the magnitude function, and $S := \{(x,y)|M(x,y) > \Gamma_g\}$ be the set of voting pixels. For each $(x,y) \in S$, its voting direction is

$$\alpha(x,y) := \frac{(I_x(x,y), I_y(x,y))}{\sqrt{I_x(x,y)^2 + I_y(x,y)^2}}$$

(3) *Compute the votes:* $V(x, y; r_{\min}, r_{\max}, \Delta) = 0$. For all pixels $(x,y) \in S$, for all $(u,v) \in A(x,y;r_{\min},r_{\max},\Delta)$, increase the vote image by the voting magnitude:

$$V(u,v;r_{\min},r_{\max},\Delta) = V(u,v;r_{\min},r_{\max},\Delta) + M(x,y)$$

(4) *Update the voting direction:* For every pixel $(x,y) \in S$, find

$$(u^*, v^*) = \arg \min_{(u,v) \in A(x,y;r_{\min},r_{\max},\Delta)} V(u,v;r_{\min},r_{\max},\Delta)$$

Let $d_x = u^* - x, d_y = v^* - y$, and

$$\alpha(x,y) = \frac{(d_x, d_y)}{\sqrt{d_x^2 + d_y^2}}$$

(5) *Decrease the angular range:* $n := n - 1$. If $n > 0$ then set $\Delta := \Delta_n$ and repeat steps 3-5.
(6) *Extract centers of mass:* The centers can be extracted by thresholding the voting image

$$\{(x,y)|V(x,y;r_{\min},r_{\max},\Delta) > \Gamma_v\}$$

The intermediate results of the voting protocol are shown in Figure 3 for multiple overlapping objects. Figure 3(a) corresponds to the original binary images. Figures 3 (b)-(j) show the evolution of the voting landscape at each iteration of the process. In each instance, the landscape corresponding to the voted image is initially blurred, then subsequently refined and focused into an isolated signal.

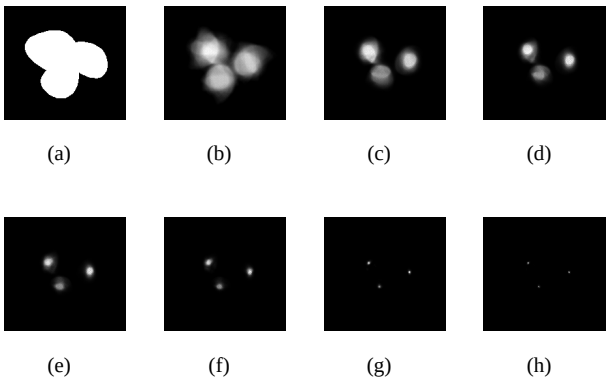

Figure 3. Clustering for radial symmetries for multiple overlapping objects: (a) original image; (b)-(j) voting landscape at each iteration.

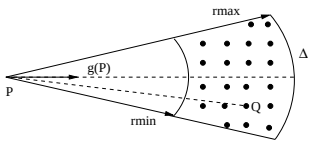

Figure 4. Reorientation of the kernel at each iteration.

3.1. Initializing voting direction and magnitude

In the absence of prior knowledge for object location, it is reasonable to assume that the center of the mass is positioned along the gradient direction. The gradient magnitude and direction can be estimated using a variety of differential operators, e.g., finite difference operators, convolution with Gaussian derivatives. The main intent is to integrate the contribution of each edge location on the grid, which may not be dense and sparsely distributed. Unlike the present practice of grouping illusory contours into a continuous representation [4], we aim at localizing gross islands of information.

3.2. Updating voting direction

Initial voting along the gradient direction provides an estimate about the position of the center of mass; however, this procedure has uncertainties associated with it, e.g., noise and deviation from strict geometric symmetry. Thus, at each consecutive iteration and each edge location, the kernel is refined and reoriented along the maximum value

in its search window as shown in Figure 4. For each point P, if Q is the maximum in P's voting area, then the new voting direction at P is along the PQ direction. In addition to low computational overhead, the rationale for associating maximum to center of mass consists of the following:

1. Under ideal conditions, the maximum value is exactly the center of mass and it hints at the most probable location, having integrated all the present boundary information.
2. By aligning the voting direction along the maximum values, local maxima, in the same neighborhood, are grouped together.

As we pointed out in the previous section, present voting techniques are limited to either a single line ($\Delta = 0$) or a constant angular range ($\Delta > 0$). Voting along a single line provides better local maxima but suffers from noise and small variations in scale. In our procedure, the angular range is gradually reduced from a large to a small number (almost 0). As a result, the voting landscape is refined and focused from coarse to fine. Eventually, the center of mass is a single isolated or a group of points that strongly clustered together. There is a strong conceptual similarity between self organizing network and the technique outlined above: (1) the size of neighborhood is allowed to vary from coarse to fine, and (2) at each iteration, local maximum (winner take all) dominates the local process.

3.3. Computational complexity

Computational and order of complexities are analyzed below. Let us examine the voting area $A(x, y; r_{\min}, r_{\max}, \Delta)$ defined by Equation 1. The cost of generating such a voting area is very high. To solve this problem, a voting direction can be quantized into angular bins, e.g.,

$$\{(\cos\frac{2\pi i}{2^n}, \sin\frac{2\pi i}{2^n}) | i = 0, 1, \cdots, 2^n - 1\}$$

such that a template voting area is generated and stored. The number of angular bins is usually set to $2^4 = 16$ or $2^5 = 32$. Compared to the voting operation, the cost of precomputing and searching these templates can be ignored. The computational complexity of each single voting is $O(K(r^2_{\max} - r^2_{\min})\Delta)$ where K is the number of pixels. If we select the sequence of angular ranges $\Delta_i = \Delta_{\max} * i/N$, then the total is

$$\sum_{i=0}^{N} K(r^2_{\max} - r^2_{\min})\Delta_{\max} i/N = O(KN\Delta_{\max}(r^2_{\max} - r^2_{\min}))$$

Essentially, the complexity is determined by the image size and geometric shapes of objects of interest. If the object is close to a circle, then $\Delta_{\max}$ and $(r^2_{\max} - r^2_{\min})$ is small, and the $O(KN\Delta_{\max}(r^2_{\max} - r^2_{\min}))$ can be as low as $O(K)$.

4. Voting Parameters

The voting algorithm contains at most five parameters. These parameters and their impacts on the voting process is summarized below:

- *Voting area:* The algorithm can be tuned to look exclusively for dark or bright objects, or both of them by selecting the signs in Equation 1. If we are interested in the bright objects, then $A(x, y; r_{\min}, r_{\max}, \Delta)$ is set to

  $$A^+(x, y; r_{\min}, r_{\max}, \Delta) := \{(x + r\cos\phi, y + r\sin\phi) | r_{\min} \le r \le r_{\max}, \theta(x, y) - \Delta \le \phi \le \theta(x, y) + \Delta\}$$

  If we are interested in dark objects, then $A(x, y; r_{\min}, r_{\max}, \Delta)$ is set to

  $$A^-(x, y; r_{\min}, r_{\max}, \Delta) := \{(x - r\cos\phi, y - r\sin\phi) | r_{\min} \le r \le r_{\max}, \theta(x, y) - \Delta \le \phi \le \theta(x, y) + \Delta\}$$

  If we want to detect objects regardless of bright/dark classifications, then bidirectional voting is needed:

  $$A^{\pm}(x, y; r_{\min}, r_{\max}, \Delta) := A^+(x, y; r_{\min}, r_{\max}, \Delta) \cup A^-(x, y; r_{\min}, r_{\max}, \Delta)$$

- *Voting magnitudes:* The voting magnitude of each pixel is always set to the gradient magnitude computed through the convolution with the derivative of a Gaussian. Small gradients corresponding to smooth surfaces are removed by introducing a gradient threshold parameter Γ_g. This threshold is set low enough so that insignificant candidates can be eliminated with high confidence. However, the end result is improved computational efficiency.
- *The radial range:* $r_{\min}$ and $r_{\max}$, and the maximum angular range $\Delta_{\max}$ $r_{\min}, r_{\max}$ and $\Delta_{\max}$ are selected by the shapes of the objects to be detected. For example, to detect a circle, we can set $r_{\min} = r_{\max}$ $\Delta_{\max} = 0$. And to detect an ellipse $\frac{x^2}{a^2} + \frac{y^2}{b^2} = 1$ one has $r_{\min} = \min(a, b), r_{\max} = \max(a, b)$ and $\Delta_{\max} =$ the maximum angle between the radial and the normal vectors (e.g., $\angle OP_1Q_1, \angle OP_2Q_2$, and $\angle OP_3Q_3$ in Figure 1) $= \arcsin\frac{|a^2 - b^2|}{a^2 + b^2}$. These are ideal cases, and tolerances will be added for real-world images.
- *Step-size in the evolution of kernel shape:* An important step of the protocol is the step-size in which the voting area/ribbon is reduced. If the step-size if too large, then centers of mass will be fragmented, and if it is too small, then the computational cost will be increased. The monotonically decreasing sequence of $\Delta_{\max} = \Delta_N < \Delta_{N-1} < \cdots < \Delta_0 = 0$ controls

the convergence rate of the algorithm. Each time the voting direction is updated, the angular range is decreased to shrink the voting area. In our system, the interval $[0, \Delta_{\max}]$ is equally partitioned and is set interactively. For an object demonstrating simple circular geometry, $N = 4$ is adequate. A higher value of N (e.g., $N = 16$) is necessary for noisy images with overlapping objects demonstrating complex geometries.

- *Threshold of output image:* The voted image (output) is always ranked. In some cases, a threshold may be set to select the most prominent set of hypotheses.

5. Experimental results

The proposed method for detecting radial symmetries has been applied to several diverse domains: (1) synthetic data demonstrating its behavior in the context of controlled noise, (2) facial data indicating its utility for man-machine interface, and (3) scientific data validating its application for meaningful representation of important events. We will show that our method is tolerant to variations in scale, has an excellent noise immunity, and can detect overlapping objects with impartial boundaries.

1. *Synthetic data:* Figure 5 shows computed localization of blobs of interest from synthetic images corrupted by noise. The boundary information of Figure 5(a) is incomplete, and the problem is one of perceptual grouping. The algorithm detects centers of the four objects successfully. Figures 5 (c)-(h) show correct detection and localization of symmetries on noisy images.
2. *Facial images:* Figure 6 shows examples of detection of circular symmetry from facial images for the purpose of man-machine interface. In all cases, the eye positions are captured and partial gradient information is clustered to infer unintended symmetries, e.g., the area between nose and lip, or lip and chin.
3. *Scientific applications:* Two groups of scientific images are provided to demonstrate extensibility of our method. The first set of data in Figure 7 originates from confocal, wide-field, and transmission electron microscopy, respectively. These images indicate that (1) blobs of interest have variable scale, (2) blobs often overlap, and (3) a significant amount of noise is often present, especially for imaging macromolecular assemblies. The second group of data, shown in Figures 8 and 9, corresponds to vortices imaged from observational platforms, scientific instruments, and output of numerical simulation models. It is assumed that an approximate measure of scale is known in advance. It is interesting to note that unlike previous results in literature, these turbulences have complex geometries, which are still captured by the proposed protocol.

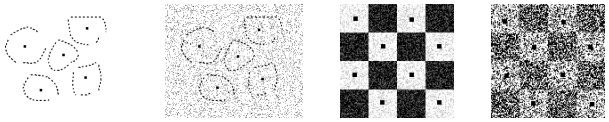

(a) (b) (c) (d)

Figure 5. Synthetic images perturbed with noise: (a-b) objects with incomplete boundaries; (c-d) checker board with increasing amount of noise.

(a) (b) (c) (d)

Figure 6. Facial images indicating detection of eye regions. In some cases, partial edges from the nose and lip contribute to local symmetries as well.

6. Conclusion and future work

We have proposed a new approach for detecting radial symmetries from nonconvex shape representations. Two new techniques are introduced: the re-estimation of voting direction and the update of voting fields from coarse to fine. The iterative and adaptive voting strategy overcomes the drawbacks of traditional static voting techniques. The method has been demonstrated on synthetic, facial, and scientific images, and shows superior performance characteristics. The limitations are as follows:

1. *Prior knowledge of scale:* Application of this algorithm assumes knowledge of scale. While this is a valid assumption for some applications (e.g., particle picking, localization of nuclei), it cannot be generalized. Thus, it is highly desirable to develop a multiscale solution to the blob detection problem.
2. *Completeness:* The method merely hypothesizes/infers potential centers of mass in each image for a given

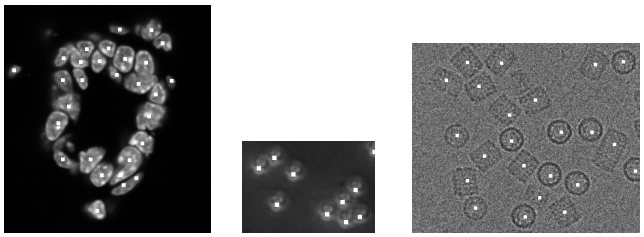

(a) (b) (c)

Figure 7. Scientific images: (a) organization of nuclei in tissue observed with a confocal microscope, (b) cells infected with the sar virus observed with wide-field microscope, and (c) macromolecular assemblies observed with a transmission electron microscope.

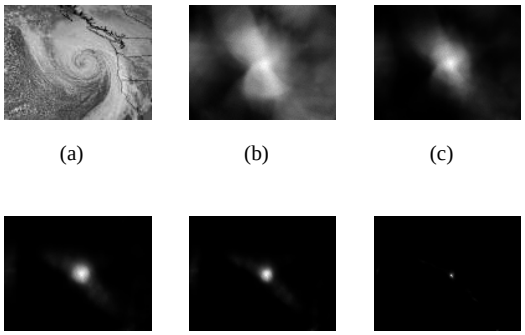

(a) (b) (c)

(d) (e) (f)

Figure 8. Localization of an atmospheric vortex: (a) original image (b-f) evolution of the voting map.

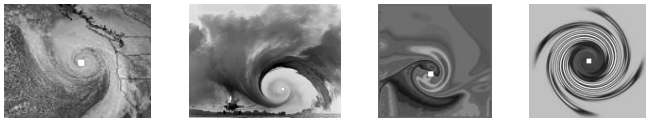

(a) (b) (c) (d)

Figure 9. Vortex detection from a variety of natural and synthetic images.

scale. These inferences need to be verified or validated by other means, which could be yet another higher-level process.

3. *Detailed delineation:* Our approach simply points to centers of mass corresponding to the circular symmetry. It is essential that such an approach be coupled with a later step to delineate object boundaries for a more accurate segmentation. Such a coupling will lead to more robust segmentation and object extraction.

References

[1] F. Attneave. Symmetry information and memory for patterns. *American Journal of Psychology*, 68:209–222, 1955.

[2] R. Duda and P. Hart. Use of the hough transform to detect lines and curves in pictures. *CACM*, 15(1):11–15, January 1972.

[3] G. Loy and A. Zelinsky. Fast radial symmetry for detecting points of interest. *PAMI*, 25(8):959–973, August 2003.

[4] G. Medioni, M. Lee, and C. Tang. *A Computational Framework for Segmentation and Grouping*. Elsevier, 2000.

[5] L. Minor and J. Sklansky. The detection and segmentation of blobs in infrared images. *SMC*, 11:194–201, 1981.

[6] D. Reisfeld, H. Wolfson, and Y. Yeshurun. Context-free attentional operators: The generalized symmetry transform. *IJCV*, 14(2):119–130, March 1995.

[7] D. Reisfeld and Y. Yeshurun. Preprocessing of face images: Detection of features and pose normalization. *CVIU*, 71(3):413–430, September 1998.

[8] G. Sela and M. Levine. Real-time attention for robotic vision. *Real-Time Imaging*, 3(3):173–194, June 1997.

[9] L. Vincent and P. Soille. Watersheds in digital spaces: An efficient algorithm based on immersion simulations. *PAMI*, 13(6):583–598, June 1991.

[10] Q. Yang and Parvin. Harmonic cut and regularized centroid transform for localization of subceullar structures. *IEEE Transaction on Biomedical Engineeing*, 50(4):469–475, April 2003.